Journal of Thermoplastic Composite Materials

http://jtc.sagepub.com

Beam Finite Element for Analyzing Free Edge Delaminations

Marco A. Pinheiro and Bhavani V. Sankar

Journal of Thermoplastic Composite Materials 2000; 13; 272
DOI: 10.1177/089270570001300402

Beam Finite Element for Analyzing Free Edge Delaminations

MARCO A. PINHEIRO[1] AND BHAVANI V. SANKAR[2]
Department of Aerospace Engineering,
Mechanics & Engineering Science
P.O. Box 116250
University of Florida
Gainesville, FL 32611-6250

ABSTRACT: A method is proposed to obtain the strain energy release rate and the stresses ahead of the crack in a laminated composite plate due to free edge delamination under Mode I type loading situations. A shear deformable beam finite element with nodes offset to either the top or bottom side has been developed. The thermal effects originating from the curing process are included in the formulation of the problem. Two different methods are used to calculate the strain energy release rate. The first method uses the J-integral evaluated around a zero-area path surrounding the cracktip and the strain energy release rate is expressed in terms of the force and moment resultants in the elements surrounding the crack-tip. The second method is similar to the virtual crack closure method, and the strain energy release rate is expressed in terms of the forces transmitted by a rigid element placed at the crack-tip and the displacements of the nodes behind the crack-tip. The stresses ahead of the crack are obtained by using discrete spring elements in the uncracked portion of the beam. The results calculated are in good agreement with results obtained from other studies of the same problem. The advantage of the present method lies in its simplicity; in addition it requires less computational effort than the methods that use solid elements.

INTRODUCTION

THE OCCURRENCE OF delamination in free edges has been receiving increasing attention from investigators in their effort to understand and prevent delaminations in composite structures. The reason is the presence of high interlaminar stresses, especially peel stresses, in the neighborhood of a free boundary. Often the free edge problem is modeled by a plate subjected to a uniform axial strain ($\varepsilon_{xx} = \varepsilon_0$) as shown in Figure 1. During the usual fabrication process, the composite material is subjected to temperatures of several hundred degrees and

[1]Graduate Student, presently with Instituto Militar de Engenharia, Rio de Janeiro, RJ 22290, Brazil.
[2]Author to whom correspondence should be addressed.

0892-7057/00/04 0272–20 $10.00/0

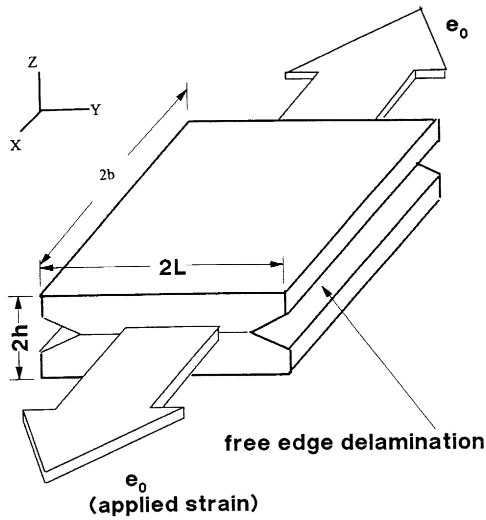

Figure 1. *The free edge problem.*

then cooled down to room temperature. The change in temperature causes thermal residual stresses, which may add to the severity of free edge stresses.

A simple procedure is developed in this study to obtain an approximate solution for the peel stresses ahead of the crack tip and also to calculate the total strain energy release rate, G, for the case of free delaminations including thermal effects. Since the present method uses the one-dimensional plate theory, it cannot separate the contributions from different modes of fracture. The problem is modeled using a shear deformable beam finite element with offset nodes (Sankar, 1991). Several assumptions are made to simplify the problem so as to use beam finite elements. First, the three-dimensional problem is approximated as a plane problem in the yz-plane assuming that the stresses and strains do not vary along the x-direction. This will be true for regions far removed from the points of load applications ($x = \pm b$ in Figure 1). Thus, the problem has been reduced to two dimensions in the yz-plane. In fact, several authors have used such an approximation. Pipes and Pagano (1970) modeled the free edge stress problem as a plane elasticity problem and solved it using the finite difference method. In the present study, we further simplify the problem as one dimensional by assuming that the plate is in a state of plane stress parallel to the xy-plane (usual laminated plate theory assumption). Thus, we consider the variation of displacements and rotation along the y-direction only, thereby reducing the problem to that of a one-dimensional plate (sometimes referred to as a beam), which can be solved using modified beam finite elements.

The delamination plane divides the laminate into two parts, the top sublaminate and the bottom sublaminate (Figure 2), which are modeled using beam finite elements with nodes offset to the bottom and top, respectively. It is assumed that the delamination plane is the weakest one, and the crack propagation would occur along this plane without crack branching. Two different models are used in the present study. When the energy release rate is calculated, the top and bottom laminates in the uncracked region of the beam have common nodes, except at the tip of the crack, where a rigid element is used to connect the top and bottom nodes (Figure 3). This rigid element not only ensures the continuity of displacements and rotations at that section, but also brings in its formulation the generalized forces that are transmitted between the sublaminates. These forces are used in the calculation of G. For the purpose of computing the peel stresses ahead of the crack, the uncracked region of the beam is connected by spring elements (Figure 4), the stiffness of which has to be judiciously selected.

In this study, the strain energy release rate G is obtained from two different methods (Sankar and Pinheiro, 1990; Sankar, 1991). The first method uses the J-integral evaluated around a zero-area path surrounding the crack tip, and the strain energy release rate is expressed in terms of the force and moment resultants in the elements surrounding the crack-tip. The second method is similar to the virtual crack closure method, and the strain energy release rate is expressed in terms of the forces transmitted by a rigid element placed at the tip of the crack and the displacements of the nodes behind the crack tip. The results from the two different methods are found to be in good agreement with available results. The agreement between the two methods itself is not surprising because they are interrelated (Sankar, 1991).

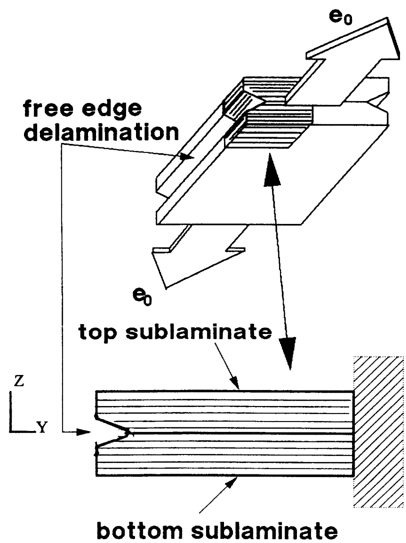

Figure 2. *Beam model of the free-edge problem.*

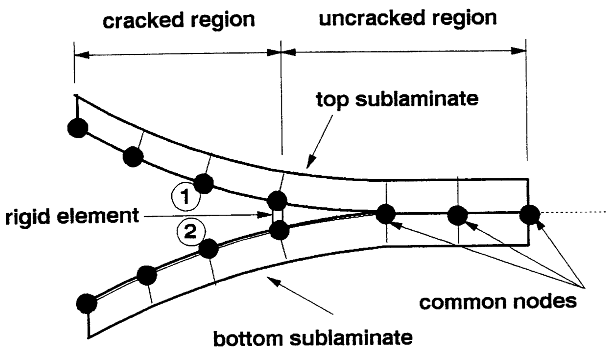

Figure 3. *Finite element model for calculation of* G.

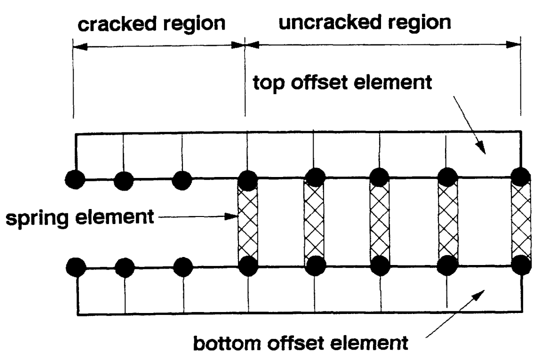

Figure 4. *Finite element model for calculation of interlaminar normal stresses.*

ONE-DIMENSIONAL LAMINATED PLATE EQUATIONS

In this section, a laminated plate subjected to a uniform initial strain $\varepsilon_{xx} = e_0$ (Figure 1) is analyzed. The thickness of the laminate is $2h$, and the width is $2b$. It is assumed that $2h$ is much smaller than $2L$ and that $2L$ is much smaller than $2b$ (Figures 1 and 2). We assume symmetry about the xz-plane and analyze only one half of the laminate (right of the xz-plane). It should be noted that the individual layers may not be symmetric with respect to the xz-plane. However, we are using the plate theory, and hence it is sufficient that the kinematic variables in the plate theory are symmetric. In the following, the reference xy-plane for the laminate is assumed to be situated at either the top or bottom surface of the sublaminates. Thus, the resultant moments and also the $[A]$, $[B]$ and $[D]$ matrices refer not to the midplane but to the reference plane which is offset from the middle plane. Hence, we use the notation $[a]$, $[b]$ and $[d]$ for the laminate stiffness to differentiate them from the conventional laminate stiffness matrices. For example, the stiffness coefficients of a laminate situated just above the xy-plane are given by the following:

$$(a_{ij}, b_{ij}, d_{ij}) = \int_0^h \bar{Q}_{ij}(1, z, z^2)\, dz, \quad (i, j = 1, 2, 6) \tag{1}$$

where h is the half-laminate thickness. The equations derived in the next section refer to a laminated beam situated above the delamination plane. The expressions for the laminated beam situated below the delamination plane differ only in the integration limits, $-h$ to 0 instead of 0 to h.

The problem is divided into two different phases. In the first phase, no external load is applied to the laminate, which is subjected only to thermal stresses due to the curing process. In the second phase, the cured specimen containing the edge delaminating is subjected to the axial strain $\varepsilon_{xx} = e_0$ in addition to the residual thermal stresses.

Thermal Stresses

During the composite fabrication process, the laminate is cooled from a higher temperature at which it is stress-free to room temperature. This causes residual stresses in the composite plate. The thermal stress problem is a standard one, analysis of which can be found in any textbook on composites, e.g., Agarwal and Broutman (1990). The derivation of laminate equilibrium equations in this study is identical to the conventional procedure, except for the limits of integration in evaluating the force and moment resultants and the laminate stiffness coefficients, because the delaminating plane is used as the reference plane. The limits should be 0 and h for a laminate above the reference plane, and $-h$ and 0 for a laminate below the reference plane. The fictitious thermal force and moment resultants are applied as external forces in the finite element model to compute the displacements. The details of the derivations can also be found in Pinheiro (1991).

Free Edge Problem

In analyzing the free edge problem, we assume that the laminate is subjected to linearly varying displacements in the x-direction:

$$u(x,y,z) = e_0 x \tag{2}$$

such that

$$\varepsilon_{xx} = e_0 \tag{3}$$

The effect of this axial strain will be represented as equivalent forces and couple acting on the beam as follows. The stress-strain relations for the kth layer are as follows:

$$\begin{pmatrix} \sigma_{xx} \\ \sigma_{yy} \\ \tau_{yz} \end{pmatrix} = \begin{bmatrix} \bar{Q}_{11} & \bar{Q}_{12} & 0 \\ \bar{Q}_{12} & \bar{Q}_{22} & 0 \\ 0 & 0 & \bar{Q}_{44} \end{bmatrix} \begin{pmatrix} e_0 \\ \varepsilon_{yy} \\ \gamma_{yz} \end{pmatrix} \tag{4}$$

The axial force P, bending moment M, and shear force V acting on the top sub-laminate are defined as

$$(P, M, V) = \int_0^h (\sigma_{yy}, z\sigma_{yy}, \tau_{yz})\, dz \tag{5}$$

From Equations (4) and (5) and also using the laminate stiffness definition given in Equation (1), the beam constitutive relations take the form

$$\begin{pmatrix} P \\ M \\ V \end{pmatrix} = \begin{bmatrix} a_{22} & b_{22} & 0 \\ b_{22} & a_{22} & 0 \\ 0 & 0 & a_{44} \end{bmatrix} \begin{pmatrix} \varepsilon_{yy}^0 \\ \kappa_{yy} \\ \gamma_{yz}^0 \end{pmatrix} - \begin{pmatrix} P_0 \\ M_0 \\ 0 \end{pmatrix} \tag{6}$$

where a_{44} is the transverse shear stiffness defined as

$$a_{44} = \kappa^2 \int_0^h \bar{Q}_{44} dz \tag{7}$$

The shear correction factor κ^2 is taken as 5/6 in the present study. In Equation (6), ε_{yy}^0, γ_{yz}^0 and κ_{yy} are the mid-plane axial strain, transverse shear strain, and curvature, respectively, and P_0 and M_0 are the equivalent force and moment that represent the effects of the applied strain e_0. They are defined as

$$(P_0, M_0) = -e_0 \int_0^h \bar{Q}_{12}(1, z) dz = -e_0 (a_{12}, b_{12}) \tag{8}$$

The thermal force and moment resultants discussed in the last section can also be added to Equation (6) to obtain

$$\begin{pmatrix} P \\ M \\ V \end{pmatrix} = \begin{bmatrix} a_{22} & b_{22} & 0 \\ b_{22} & a_{22} & 0 \\ 0 & 0 & a_{44} \end{bmatrix} \begin{pmatrix} \varepsilon_{yy}^0 \\ \kappa_{yy} \\ \gamma_{yz}^0 \end{pmatrix} - \begin{pmatrix} P_0 \\ M_0 \\ 0 \end{pmatrix} - \begin{pmatrix} P_T \\ M_T \\ 0 \end{pmatrix} \tag{9}$$

In the shorthand notation, Equation (9) can be written as

$$\underline{F} = \underline{S}\,\underline{e} - \underline{R} \tag{10}$$

where $\underline{S}$ is the laminate stiffness matrix, components of which are

$$\underline{S} = \begin{bmatrix} a_{22} & b_{22} & 0 \\ b_{22} & a_{22} & 0 \\ 0 & 0 & a_{44} \end{bmatrix} \tag{11}$$

and $\underline{R}$ is the vector that represents the forces and moments induced by the applied strain as well as the thermal effects:

$$\underline{R}^T = \lfloor P_T \quad M_T \quad 0 \rfloor + \lfloor P_0 \quad M_0 \quad 0 \rfloor \tag{12}$$

In Equation (12) and also what follows, an underscore represents a matrix, and a superscript T denotes matrix transpose. The vectors $\underline{F}$ and $\underline{e}$ are defined as follows:

$$\underline{F}^T = \lfloor P \quad M \quad V \rfloor \tag{13}$$

$$\underline{e}^T = \lfloor \varepsilon_{yy}^0 \quad \kappa_{yy} \quad \gamma_{yz}^0 \rfloor \tag{14}$$

Finally, Equation (10) can also be expressed as

$$\underset{\sim}{e} = \underset{\sim}{C}(\underset{\sim}{F} + \underset{\sim}{R}) \tag{15}$$

where $C = S^{-1}$ is the compliance matrix.

FINITE ELEMENT SOLUTION

The laminate with the free edge delaminating is modeled by two types of beam finite elements. The top sublaminate, which is above the plane of delaminating, is modeled using finite elements with nodes offset to the bottom side. The bottom sublaminate is modeled by elements with nodes offset to the top. In the uncracked region, the two sets of elements are connected by spring elements or share common nodes depending on the calculation performed. In the delaminated portion, one can use gap elements, if necessary, to monitor the contact between delaminated surfaces.

The finite element has two nodes and three degrees of freedom, namely, axial displacement, rotation about the x-axis, and transverse displacement, (v, ψ, and w) at each node. The generalized nodal forces at the ith node are denoted by f_{yi}, m_i and f_{zi}. In what follows, we describe a novel procedure to derive the element stiffness matrix. The force and moment resultants (P, M and V) at the center of the element can be approximated using linear interpolation as

$$\begin{pmatrix} P \\ M \\ V \end{pmatrix} = \begin{pmatrix} (f_{y2} - f_{y1})/2 \\ (m_2 - m_1)/2 \\ (f_{z2} - f_{z1})/2 \end{pmatrix} \tag{16}$$

It should be noted that the force and moment resultants and the generalized nodal forces have different sign conventions, and that is the reason for the negative signs in Equation (16). The nodal forces are vectors that follow the sign convention of the coordinate axes, e.g., the force f_z acting in the positive z-direction is positive, whereas a positive z-force acting at the left end of the beam will create a negative shear force resultant V. In expressing the force and moment resultants at the center of the element in terms of the nodal values, we have used a linear variation of these quantities along the length of the element. The average deformations at the center of the element are expressed in terms of the nodal displacements as

$$\underset{\sim}{e} = \begin{pmatrix} \varepsilon_{yy}^0 \\ \kappa_{yy} \\ \gamma_{yz}^0 \end{pmatrix} = \begin{pmatrix} (v_2 - v_1)/a \\ (\psi_2 - \psi_1)/a \\ (\psi_2 + \psi_1)/2 + (w_2 - w_1)/a \end{pmatrix} \tag{17}$$

where a is the element length. In deriving Equation (17), we have assumed a first order approximation for the derivatives. In other words, a linear variation of the displacement variables is inherently assumed. Further, in deriving the last term in Equation (17), we have used the definition of the shear strain

$$\gamma_{yz}^{0} = \psi + \frac{\partial w}{\partial x}$$

Now we require that the average force resultants and the deformations satisfy the laminate constitutive relations given by Equation (16), which yields three equations between the nodal forces and displacements. The remaining three equations are obtained from the fact that the nodal forces should satisfy static equilibrium. From the six equations, the relation between nodal forces and displacements is obtained in the form

$$\underline{f} = \underline{k}\underline{q} - \underline{f}_0 \tag{18}$$

where $\underline{k}$ is the element stiffness matrix, and $\underline{f}$, $\underline{q}$, and $\underline{f}_0$ are the vectors of nodal forces, nodal displacements, and residual forces, respectively:

$$\underline{f}^T = \lfloor f_{y1} \quad m_1 \quad f_{z1} \quad f_{y2} \quad m_2 \quad f_{z2} \rfloor \tag{19}$$

$$\underline{q}^T = \lfloor v_1 \quad \psi_1 \quad w_1 \quad v_2 \quad \psi_2 \quad w_2 \rfloor \tag{20}$$

$$\underline{f}_0^T = \lfloor -\underline{R}^T \quad \underline{R}^T \rfloor \tag{21}$$

The vector $\underline{R}$ and its components are defined by Equation (12). The explicit expressions for the element stiffness matrix $[k]$ are given in Appendix A. A detailed derivation of the stiffness matrix can be found in Pinheiro (1991). It may be noted that in the present formulation, energy methods have not been used to derive the stiffness matrix. The equilibrium equations and constitutive relations are directly satisfied. Hence, there is no shear locking in this element (Sankar, 1991).

Strain Energy Release Rate

It may be noted that the thermal stress problem is being solved by superposing two problems. The first problem is a trivial one in which the displacements are zero but stresses exist because of the constraint on thermal expansion. In the second problem, the thermal forces are reversed and applied as external forces. From the fracture mechanics perspective, there is no singularity in the first problem, and hence no stress intensity factor or strain energy release rate exists. The strain energy release rate values calculated in the second problem represent the G for the free edge delamination problem.

In computing the strain energy release rate, a rigid element is placed at the tip of the crack connecting both sublaminates (Figure 3). The rigid element has nine degrees of freedom. Apart from the three displacements at each node, the three generalized forces, F_t, transmitted by the rigid element are also considered as unknown degrees of freedom. The constraint equations corresponding to the rigid element are

$$\begin{pmatrix} f_1 \\ f_2 \\ 0 \end{pmatrix} = \begin{bmatrix} 0_3 & 0_3 & -I_3 \\ 0_3 & 0_3 & I_3 \\ -I_3 & I_3 & 0_3 \end{bmatrix} \tag{22}$$

where $\underline{f}_1$ and $\underline{f}_2$ are the vector of nodal forces at nodes 1 and 2, and $\underline{q}_1$ and $\underline{q}_2$ are the vector of nodal displacements. The symbol 0_3 represents the 3×3 null matrix and I_3 the 3×3 identity matrix.

The procedures for computing the strain energy release rate using beam finite elements can be found in Sankar (1991). A brief description is given here for the sake of completion. Considering a zero volume path surrounding the crack tip as shown in Figure 5, and knowing that for linear elastic fracture the J-integral is equivalent to the energy release rate (Hellan, 1984), the expression for G is given by

$$G = J = J_1 + J_2 + J_3 + J_4 \tag{23}$$

where J represents the J-integral value corresponding to the ith sublaminate (Figure 5). Substituting for the terms in the J-integral in terms of the strains, we obtain (Sankar, 1991):

$$J = \frac{1}{2}(\underline{e}_1^T \underline{S}_b \underline{e}_1 + \underline{e}_4^T \underline{S}_t \underline{e}_4 - \underline{e}_2^T \underline{S}_b \underline{e}_2 - \underline{e}_3^T \underline{S}_t \underline{e}_3) \tag{24}$$

where $\underline{e}_i$ is the deformation in the ith sublaminate, and $\underline{S}_t$, and $\underline{S}_b$ are the stiffness matrices on the top and bottom sublaminates respectively as defined in Equation (11). The strain energy release rate can also be expressed in terms of the force and moment resultants in the sublaminate as follows (Sankar, 1991):

$$G = \frac{1}{2}(\underline{F}_1^T C_t \underline{F}_1 + \underline{F}_4^T C_b \underline{F}_4 - \underline{F}_2^T C_t \underline{F}_2 - \underline{F}_3^T C_b \underline{F}_3) \tag{25}$$

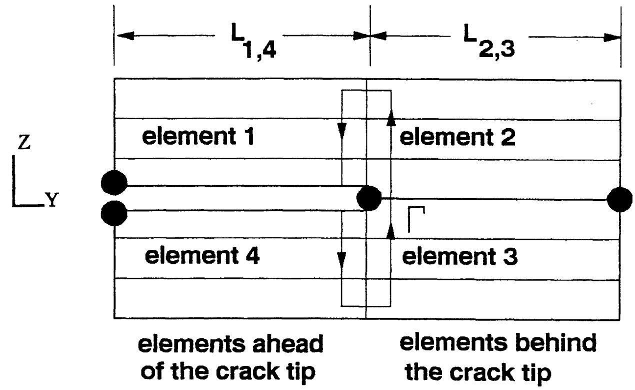

Figure 5. *Zero-volume path for the J-integral.*

where the force and moment resultants F_i $(i = 1, \ldots 4)$ are calculated from the finite element solution. In Equation (25) C_t and C_b are the compliance matrices of the top and bottom sublaminates [see Equation (15)]. The elements 2 and 3 (Figure 5) are in the uncracked region, so they are under the same deformations. We thus obtain the following relations:

$$\underline{e}_2 = \underline{e}_3 \tag{26}$$

$$\underline{C}_t \underline{F}_2 = \underline{C}_b \underline{F}_3 \tag{27}$$

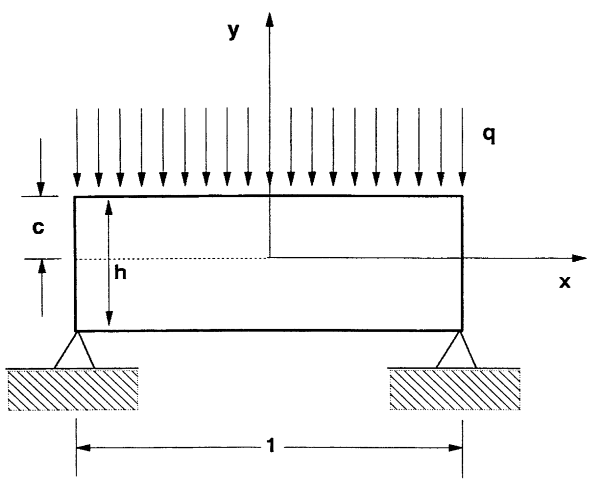

Figure 6. *Beam model for estimating the foundation spring constant.*

Substituting Equations (26) and (27) and also using the equilibrium relations $F_1 + F_4 = F_2 + F_3$ in Equation (25), we obtain

$$G = \frac{1}{2}(\underline{F}_1 - \underline{F}_2)^T(\underline{C}_t + \underline{C}_b)(\underline{F}_1 - \underline{F}_2) \tag{28}$$

Actually, $(\underline{F}_1 - \underline{F}_2)$ is the force transmitted by the rigid element between the bottom and top crack tip nodes. Therefore, the strain energy release rate (G) can be expressed in a more convenient form as

$$G = \frac{1}{2}\underline{F}_r^T(\underline{C}_t + \underline{C}_b)\underline{F}_r \tag{29}$$

In the above equation $\underline{F}_r$, is the vector of forces and couple transmitted by the rigid element, which is part of the finite element solution of the problem.

One can also evaluate the value of the strain energy release rate using a method analogous to the virtual crack closure method in two-dimensional fracture problems (Hellan, 1984). In this method, the energy necessary to close the crack is equal to the energy release rate. The expression for G that results from this method is (Sankar, 1991)

$$G = \frac{1}{2a}\underline{F}_r^T(\underline{q}_1 - \underline{q}_2) \tag{30}$$

where a is the length of the crack tip elements, i.e., the four elements connected to the crack tip, and q_1 and q_2 are the displacements of Nodes 1 and 2 as shown in Figure 3. Thus, the strain energy release rate can be computed by either Equation (29) or Equation (30). In fact, we obtained identical results using both equations.

Stresses Ahead of the Crack Tip

Even though the strain energy release rate can be used as a criterion for the propagation of delaminations, some researchers have used average stresses ahead of the crack tip as a criterion for failure. Thus, the crack-tip stresses may be of some interest. Strictly speaking, the stresses near the crack tip are singular; however, if one is interested in stresses averaged over a given length, then approximate methods can be used to estimate the stresses. In evaluating the stresses ahead of the crack tip, the nodes of the top and bottom sublaminate of the uncracked region were connected by discrete spring elements (Figure 4). The σ_{zz} stresses ahead of the crack tip were computed as

$$\sigma_{zz} = \frac{F_s}{ab} \tag{31}$$

where F_s is the spring force, a is the length of the element ahead of the crack-tip, and b is the beam width (unity in the present case).

The determination of the spring constant for the spring elements is significant in appropriately modeling the problem. Actually, the spring represents the elastic foundation of the beam. Kanninen (1985) used a spring constant equal to $2E/h$, where E is the Young's modulus and h is the thickness of the top or bottom beam. In the present study, we used a more accurate approach (Appendix B) to estimate the spring constant of the foundation as

$$k = \frac{32E^*}{13h} \tag{32}$$

where E^* is the effective Young's modulus in the thickness direction, and h is the beam thickness. Considering the top and bottom sublaminates, we have two springs placed in series, and hence the equivalent spring constant k can be expressed as

$$k_{eq} = \frac{32E^*}{13(h_t + h_b)} \tag{33}$$

where the subscripts t and b stand for top and bottom sublaminates respectively.

RESULTS AND DISCUSSION

Some results for the strain energy release rate and the interlaminar stresses in a free edge specimen can be found in Whitney (1986), Pagano (1989), and Raju (1986). These researchers computed results for the same composite specimen, which is also used in the present study. Whitney and Pagano used a higher order laminated plate theory which includes transverse shear deformation and a thickness-stretch mode. The governing plate differential equations were solved in closed-form to obtain solutions for deflections and stresses ahead of the crack tip. The strain energy release rate was obtained by differentiating the compliance of the specimen with respect to crack length. Raju used quasi-three-dimensional finite elements in conjunction with a crack closure method to compute the strain energy release rate.

The free-edge specimen width-to-thickness ratio (L/h) is 25, which is typical for conventional edge delamination test (EDT) specimens. The ply properties are $E_1/E_2 = 14$, $E_2/E_3 = 1$, $G_{12}/E_2 = 0.533$, $G_{23}/E_2 = 0.323$, $\nu_{12} = 0.3$, $\nu_{23} = 0.55$, $\alpha_1 = -9 \times 10^{-7}/°C$, $\alpha_2 = \alpha_3 = 9 \times 10^{-7}/°C$, where the 1-direction is parallel to the fibers and the 3-direction is parallel to the z-axis. The thermal expansion coefficients in the x_i direction are denoted by α_i. These properties and relations among them are typical of current high-performance graphite/epoxy unidirectional composites.

The specimens considered in the present study have the following lay-ups: Specimen A: $[90_3/0_3]_s$; Specimen B: $[-60/60_2/-60/0_2]_s$; Specimen C: $[-45/45_2/-45/0_2]_s$; Specimen D: $[0_2/-60/60_2/-60]$. A reasonable value for stress-free temperature for standard graphite/epoxy laminates is 138°C (280°F) (Whitney, 1986). Assuming 21°C (70°F) as the room temperature, the difference in temperature (ΔT) that causes residual stresses in the plies is equal to −117°C (210°F). The critical axial strains (e_0) experimentally determined in edge delamination tests are 0.3% for angle-ply laminates (Whitney, 1986). These are the values of strains used in the numerical examples.

The normalized strain energy release rate, G_N, is given by

$$G_N = \frac{G}{E_2 h e_0^2} \tag{34}$$

The results obtained from the present method—using either of Equations (29) or (30)—are compared with available results in Table 1. The numbers in parentheses indicate the percent difference between the corresponding result and that obtained by the present method.

From Table 1 it can be seen that the present results compare very well with Raju (1986) for all laminate configurations considered, whereas the comparison with the other two methods is good in most cases. It should be mentioned that of the three methods we compared, Raju (1986) used a detailed finite element analysis

Table 1. Comparison of strain energy release rate (G) from different methods. G is in J/m^2. Numbers in parentheses indicate percent difference between the present results and others.

Laminate	ε (%)	ΔT (°C)	Whitney	Raju	Present
$[-60/60_2/-60/0_2]_s$	0.3	0	1.300 (0.0)	1.251 (4.0)	1.300
	0.3	−117	1.700 (21.6)	1.955 (5.3)	2.058
$[0_2/-60/60_2/-60]_s$	0.3	0	1.300 (0.0)	1.270 (2.4)	1.300
	0.3	−117	1.000 (−28.4)	0.670 (6.9)	0.7160
$[90_3/0_3]_s$	1.0	0	0.016 (2.5)	0.0155 (0.6)	0.0156
	1.0	−117	0.077 (−15.6)	0.0605 (0.0)	0.0650
$[-45/45_2/-45/0_2]_s$	0.3	0	0.770 (−3.4)	0.7285 (2.1)	0.744
	0.3	−117	0/800 (8.0)	0.9194 (−6.0)	0.864

using quasi-three-dimensional parabolic elements. It may be noted that both the present method and the method used by Whitney use approximate plate theories to model the free edge delaminations; hence, they are bound to differ from that of the detailed finite element solution. However, we are able to obtain a good engineering solution with far less computational effort. In the present method, we have used about twenty beam elements to model the free edge delaminating. It should be noted that the results obtained in the present study do not depend on the crack length. This situation is similar to the case of a double cantilever beam subjected to equal and opposite end moments at each of the cracked ligaments, where the *G* depends not on the crack length, but only on the magnitude of the end moments.

The interlaminar normal stresses ahead of the crack tip are evaluated using spring elements in the uncracked region of the specimen. The spring constant for these elements is calculated by Equation (33) and found to be equal to 300 × 10^9 N/m. Figures 7–10 show the results for peel stresses for different laminate configurations, with and without thermal effects. In Figure 7, the stress distribution is compared with Whitney (1986) for $\Delta T = 0°C$ and $\Delta T = -117°C$ for the specimen B ($[-60/60_2/-60/0_2]_s$), and the agreement is excellent. From the results, we find that the effect of residual thermal stresses is an increase in the maximum peel stress at the free edge. The effect is significant for Specimen A ($[90_3/0_3]_s$), and less significant for Specimen C ($[-45/45_2/-45/0_2]_s$). This may be because in Specimen C the

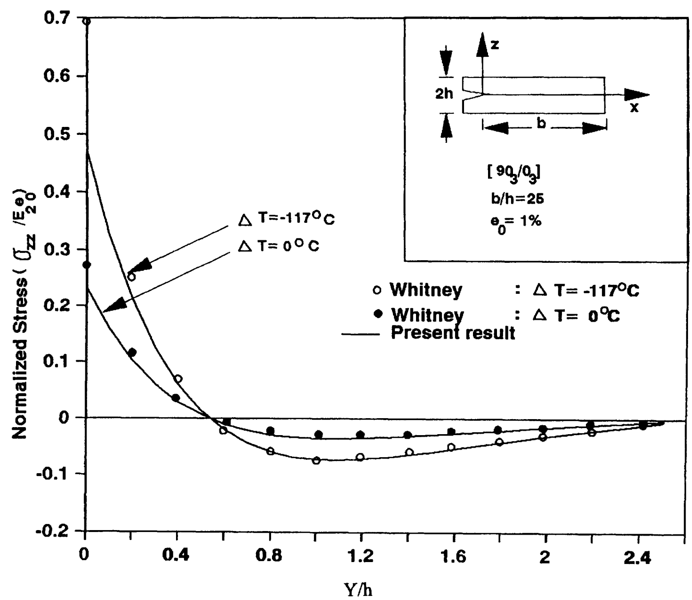

Figure 7. *Normal stresses ahead of the crack tip for Specimen A.*

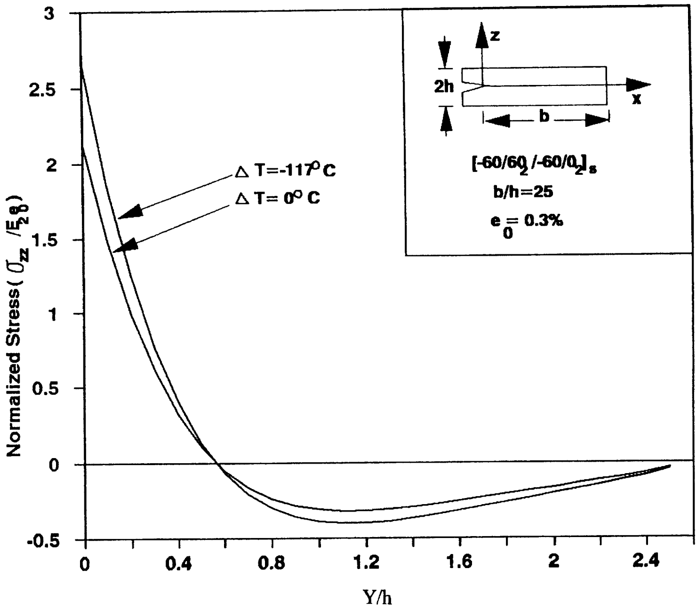

Figure 8. *Normal stresses ahead of the crack tip for Specimen B.*

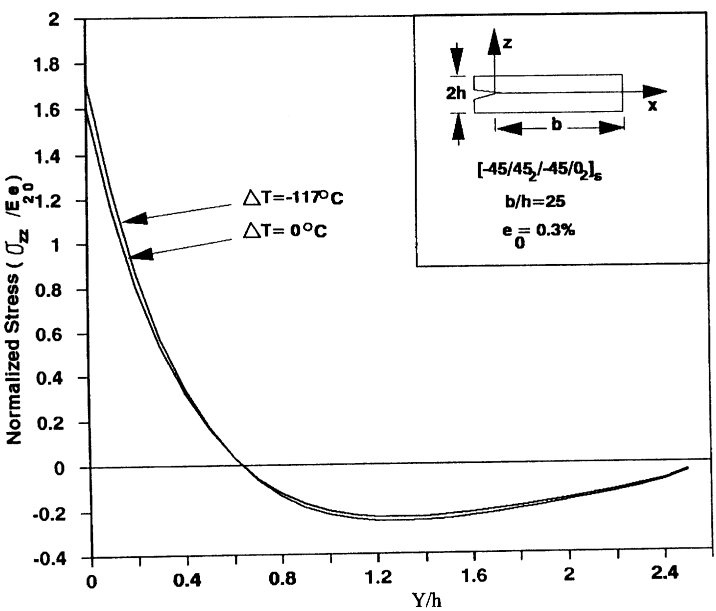

Figure 9. *Normal stresses ahead of the crack tip for Specimen C.*

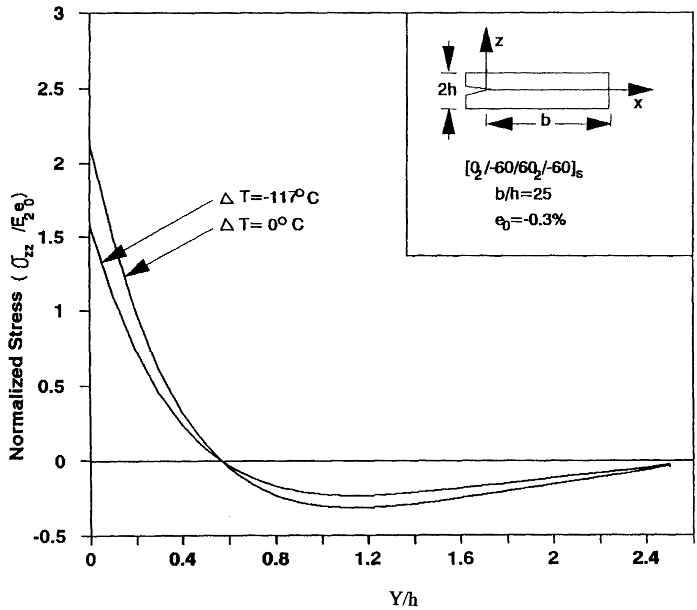

Figure 10. *Normal stresses ahead of the crack tip for Specimen D.*

layers are more dispersed than in Specimen A, in which the 0- and 90-degree layers appear in block. Thus, Specimen C exhibits more homogeneity and hence less thermal residual stress effect than Specimen A.

SUMMARY

A shear deformable beam finite element with nodes offset to the top and bottom sides of the beam is used to model the free-edge delaminating problem. The strain energy release rate has been computed from the force and moment resultants in the sublaminates surrounding the crack tip. A foundation spring model is used to estimate the peel stresses ahead of the crack tip. The results are in good agreement with available results for various laminate configurations including the effects of thermal stresses due to the curing process.

ACKNOWLEDGEMENT

This research was partially supported by a grant from the Florida Space Grants Consortium under the Florida Space Research Program. The first author (MAP) wishes to acknowledge the support from the Brazilian Army and the National Research Council of Brazil.

APPENDIX A

The non-zero coefficients of the 6 × 6 symmetric stiffness matrix $[k]$ of a beam finite element with offset nodes are given below. The nodes are situated on the bottom side of the laminate, i.e., z is positive everywhere in the laminate. The element length is l, and the width in the x-direction is assumed to be unity. The degrees of freedom in the appropriate order are v_1, ψ_1, w_1, v_2, ψ_2 and w_2. $k_{11} = a_{11}/l$, $k_{12} = b_{11}/l$, $k_{14} = -k_{11}$, $k_{15} = -k_{12}$, $k_{22} = d_{11}/l + a_{55}l/4$, $k_{23} = -a_{55}/2$, $k_{24} = k_{15}$, $k_{25} = -d_{11}/l + a_{55}l/4$, $k_{26} = a_{55}/2$, $k_{33} = a_{55}/l$, $k_{35} = k_{23}$, $k_{36} = -k_{33}$, $k_{44} = k_{11}$, $k_{45} = k_{12}$, $k_{55} = k_{22}$, $k_{56} = k_{26}$, $k_{66} = k_{33}$.

For a laminate with nodes offset to the top, i.e., z is negative in the entire laminate, the element stiffness matrix can be obtained by appropriate coordinate transformation.

APPENDIX B

A simple procedure for determining the foundation constants is explained in this section. Consider an isotropic beam subjected to uniformly distributed forces (Figure 6). Following Timoshenko and Goodier (1970), we have, for this case

$$\varepsilon_{yy} = -\frac{3q}{4c^3E^*}\left(\frac{1}{2}y^3 - c^2y + \frac{2}{3}c^3\right) \tag{35}$$

where E^* is defined as

$$E^* = \frac{E}{1 - \nu^2} \tag{36}$$

The vertical displacement (v) is obtained by integrating the deformation ε_{yy} in the y-direction. The result is

$$v = \int \varepsilon_{yy} dy = -\frac{3q}{4c^3E^*}\left(\frac{y^4}{12} - \frac{c^2y^2}{2} + \frac{2}{3}c^3y\right) + C_1 \tag{37}$$

where C_1 is a constant. From Equation (37), the displacements at the positions $y = -c$ and $y = 0$ are determined as

$$v(-c) = \frac{13}{16}\frac{qc}{E^*} + C_1 \tag{38}$$

$$v(0) = C_1 \tag{39}$$

and the relative displacement between these two particular positions as

$$v_R = v(-c) - v(0) = \frac{13}{16}\frac{qc}{E^*} \tag{40}$$

For a beam element of unit length and unit width, the total load $P = q$. In the present case, c is equal to half the thickness of the beam ($c = h/2$). Therefore, Equation (40) can be rewritten as

$$P = \frac{32E^* v_R}{13h} \tag{41}$$

From Equation (41) we have the value for the spring constant per unit length as

$$k = \frac{32E^*}{13h} \tag{42}$$

It may be noted that this value is slightly higher than the conventional foundation constant $2E^*/h$. For orthotropic beams, E^* can be approximated by the Young's modulus in the thickness direction of the beam.

REFERENCES

Agarwal, B. D. and Broutman, L. J. (1990), *Analysis and Performance of Fiber Composites,* John Wiley & Sons, New York, NY.

Hellan, K. (1984), *Introduction to Fracture Mechanics,* McGraw-Hill, New York, New York, 1984.

Kanninen, M. F. (1985), *Advanced Fracture Mechanics,* Oxford University Press, New York, NY.

Pinheiro, M. A. (1991), "Finite Elements for Free Edge Delaminating and Anisotropic Delaminated Beams," Doctoral Dissertation, Department of Aerospace Engineering, Mechanics & Engineering Science, University of Florida, Gainesville, Florida.

Pagano, N. J. (1989), *Interlaminar Response of Composite Materials,* Elsevier Science Publishing Company, New York, New York.

Pipes, R. B. and Pagano, N. J. (1970) "Interlaminar Stresses in Composite Laminates under Uniform Axial Extension," *J. Composite Materials,* Vol. 4, No. 4, p. 538.

Raju, I. S. (1986), "Q3DG—A Computer Program for Strain Energy Release Rate for Delaminating Growth in Composite Laminates," NASA CR 178205.

Sankar, B. V. (1991), "A Finite Element for Modeling Delaminations in Composite Beams," *Computers & Structures,* Vol. 38, No. 2, pp. 239–246.

Sankar, B. V. and Pinheiro, M. A. (1990), "An Offset Beam Finite Element for Fracture Analysis of

Delaminations," AIAA Paper Number: AIAA-90-1024-CP. Proceedings of AIAA/ASME/ASCE/AHS/ASC 31st SDM Conference, Long Beach, California, pp. 1227–1233.

Timoshenko, S. P. and Goodier, J. M. (1970), *Theory of Elasticity,* McGraw-Hill, New York, NY, pp. 50–53.

Whitney, J. M. (1986), "Stress Analysis of Mode I Edge Delaminating Specimen for Composite Materials," *AIAA Journal,* Vol. 24, No. 7, pp. 1163–1168.

Whitney, J. M. (1987), *Structural Analysis of Laminated Anisotropic Plates,* Technomic Publishing Company, Lancaster, PA.